Existence of characteristic spectral signatures for agricultural crops – Potential for automated crop mapping by hyperspectral imaging

Article *in* Geocarto International · January 2011

DOI: 10.1080/10106049.2011.623792

CITATIONS
7

READS
1,134

2 authors:

Rama Rao Nidamanuri
Indian Institute of Space Science and Technology
75 PUBLICATIONS **799** CITATIONS

SEE PROFILE

Bernd Zbell
Leibniz Centre for Agricultural Landscape Research
24 PUBLICATIONS **397** CITATIONS

SEE PROFILE

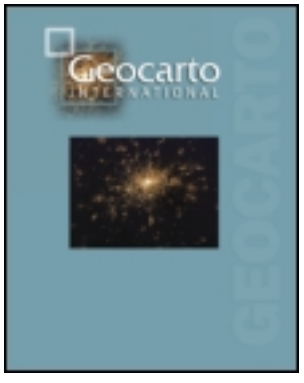

Geocarto International
Publication details, including instructions for authors and subscription information:
http://www.tandfonline.com/loi/tgei20

Existence of characteristic spectral signatures for agricultural crops - potential for automated crop mapping by hyperspectral imaging

Rama Rao Nidamanuri [a] & Bernd Zbell [b]

[a] Department of Earth and Space Sciences, Indian Institute of Space Science and Technology, Department of Space, Government of India, Valiamala P.O., Thiruvananthapuram, 695 547, India

[b] Leibniz - Centre for Agricultural Landscape Research (ZALF), Institute for Landscape SystemsAnalysis, Eberswalder str. 84, Muencheberg, 15374, Germany

Accepted author version posted online: 23 Sep 2011.Published online: 10 Nov 2011.

To cite this article: Rama Rao Nidamanuri & Bernd Zbell (2012): Existence of characteristic spectral signatures for agricultural crops - potential for automated crop mapping by hyperspectral imaging, Geocarto International, 27:2, 103-118

To link to this article: http://dx.doi.org/10.1080/10106049.2011.623792

Geocarto International
Vol. 27, No. 2, April 2012, 103–118

Taylor & Francis
Taylor & Francis Group

Existence of characteristic spectral signatures for agricultural crops – potential for automated crop mapping by hyperspectral imaging

Rama Rao Nidamanuri[a]* and Bernd Zbell[b]

[a]*Department of Earth and Space Sciences, Indian Institute of Space Science and Technology, Department of Space, Government of India, Valiamala P.O., Thiruvananthapuram – 695 547, India;* [b]*Leibniz – Centre for Agricultural Landscape Research (ZALF), Institute for Landscape Systems Analysis, Eberswalder str. 84, Muencheberg 15374, Germany*

(*Received 12 July 2011; final version received 7 September 2011*)

Image classification for material mapping using independent training data is emerging as an automated method for hyperspectral image analysis. Possibility of using independent training data for image classification depends upon material type and its spectral behaviour. Identification and spectral discrimination of materials which exhibit characteristic spectral behaviour are critical for developing hyperspectral material detection and mapping methods. We identify and evaluate characteristic reflectance signature of winter rape relative to its co-occurring crops from a hyperspectral image classification perspective. Spectral libraries developed using field reflectance measurements of agricultural crops: alfalfa, winter barley, winter rape, winter rye and winter wheat collected during four growing seasons are searched through for the classification of a HyMap image acquired for a separate site by spectral angle mapper and spectral feature fitting methods. Results indicate the existence of a characteristic spectral signature for winter rape and meaningful matching between image and field spectra, which can be used for automatic mapping of winter rape by hyperspectral imaging.

Keywords: hyperspectral remote sensing; spectral signatures; spectral angle mapper; spectral library; spectral feature fitting

1. Introduction

Hyperspectral remote sensing is a versatile tool for improved mapping and modelling of various earth surface features. Modern hyperspectral imaging systems provide spectral data with unprecedented detail. To make better use of this enhanced data capability, various methods dealing with high dimensionality and classification performance have been developed (Chang 2000, Landgrebe 2002, Kaewpijit *et al*. 2003, Camps-Valls and Bruzzone 2005, Plaza *et al*. 2005, Wang and Chang 2006, Demir and Erturk 2007, Waske and Benediktsson 2007, Ratle *et al*. 2010, Stephani *et al*. 2010). Leveraging the detailed spectral characteristics of surface categories provided by hyperspectral imaging systems, there is an increasing interest in the automation of hyperspectral image classification. A relevant development in this aspect is the knowledge transfer or semi-supervised learning-based classification method (Rajan *et al*. 2006, 2008, Bue and Merenyi 2010, Bue *et al*. 2010, Liu *et al*.

*Corresponding author. Email: rao@iist.ac.in

ISSN 1010-6049 print/ISSN 1752-0762 online

http://dx.doi.org/10.1080/10106049.2011.623792
http://www.tandfonline.com

2010). In general, a significant amount of spectral knowledge is generated in every image classification experiment. While spectral knowledge represented as training data is image specific as used in multispectral image classifications, knowledge transfer methods hinge around finding a transformation that maps the surface categories between two images. Spectral knowledge acquired in the form of training data from an image is used for classifying another image of the same or adjacent area. Land cover classification accuracies obtained from this approach are reported to be comparable with those obtained from image-based training data (Knorn *et al.* 2009). However, transferring spectral knowledge from one image to another is challenging particularly when the images are captured by different sensors, under different atmospheric conditions and capturing geometry. Further, it is presumed that hyperspectral image (source image) preserves spectral characteristics of materials and a systematic scheme transferring training data would enable classification of surface categories in other hyperspectral image (target image). While this method may produce convincing results when the source and target image have significant overlapping area, it obviously fails when the source and target images are independent. However, if the surface categories exhibit unique spectral reflectance characteristics, hyperspectral images, in principle, can be classified by spectral knowledge transfer methods irrespective of the space and time of image acquisition. An alternative emerging approach that requires unique spectral signatures of surface categories is the image classification by spectral library search. The premise behind this approach is the fact that distinctive spectral signatures of various surface categories can be compiled as a reference spectral library and surface categories in the image can be identified by spectral library search using a suitable matching algorithm. Further, the spectral signatures of materials, if they are distinctive, can be used for automatic identification and mapping of those materials across space and time using hyperspectral image (Campbell 2006).

Various authors have reported the success of compiling and using reference spectral libraries for mineral mapping (Van der Meer 2005, Clark *et al.* 2007, Kokaly *et al.* 2008, Baldridge *et al.* 2009, Kruse and Perry 2009), soil classification (Shepherd and Walsh 2002, Bojinski *et al.* 2003, Brown *et al.* 2006, Brown 2007) and urban material identification (Gomez 2002, Herold *et al.* 2004) using airborne hyperspectral imagery. With varying degrees of precision, this idea has been extended recently to vegetation classification using *in situ* reflectance measurements (Cochrane 2000, Nidamanuri *et al.* 2007, Zomer *et al.* 2009). In our previous work of analysing field reflectance characteristics of several agricultural crops (Nidamanuri and Zbell 2011), outstanding spectral reflectance characteristics for winter rape had been detected. The objective of this work was the evaluation of the existence and prospect of the reflectance characteristics of winter rape relative to its co-occurring crops for winter rape mapping by hyperspectral image classification. Multi-season canopy level reflectance measurements of agricultural crops, namely, winter rape, alfalfa, winter barley, winter rye and winter wheat which are organized as spectral libraries have been used for the classification of a HyMap airborne hyperspectral image by spectral library search using spectral angle mapper (SAM) and spectral feature fitting (SFF) methods. Results suggest the existence of a unique spectral signature for winter rape which can be used for automatic mapping of winter rape by spectral library search through independent hyperspectral image.

2. Materials and methods

2.1. Study area

Spectral data used in this research were collected from two sites located in Northeast Germany. Figure 1 shows the location of the study site. Reflectance measurements of the crops selected were collected from experimental plots of the Leibniz-Centre for Agricultural Landscape Research (ZALF), Muencheberg, Germany. Airborne hyperspectral imagery as well as ground data was acquired for the Dedelow research station of the ZALF, which is located 100 km north of the site of field reflectance measurements.

2.2. Data collection

2.2.1. Hyperspectral data acquisition and preprocessing

Airborne hyperspectral imagery was acquired on 6 May 1999 using the HyMap sensor with an extent of 6 km × 10 km along east–west flight lines. The HyMap image used in this study was captured with a pixel size of 5 m and 128 spectral bands with a bandwidth of 10–20 nm. This real-time georeferenced image was processed to account for radiometric and atmospheric corrections using the Fast Line-of-sight

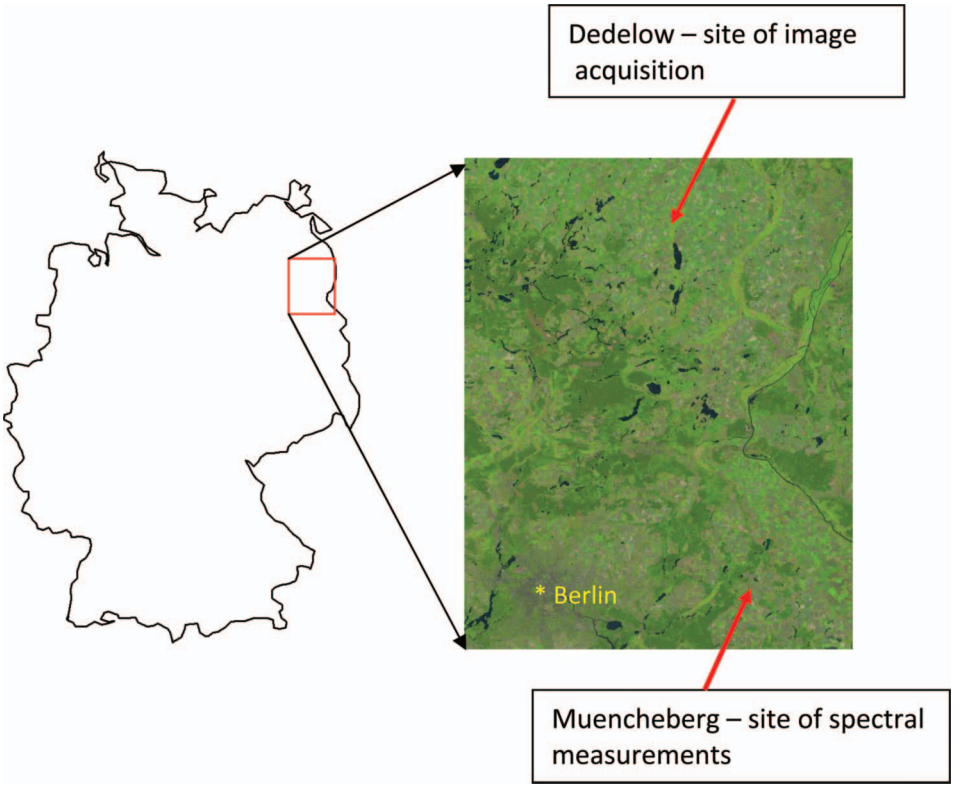

Figure 1. Location map of the study site (satellite image: True colour image of the Landsat ETM + acquired on 16 June, 2003 obtained from USGS).

Atmospheric Analysis of Spectral Hypercubes atmospheric correction code (Environment for Visualizing Images (ENVI) User Guide; Felde *et al*. 2003). Due to severe noise and low response of detecting elements, band 1 (403 nm), band 2 (447 nm), band 65 (1410 nm) and band 128 (2480 nm) were eliminated from the analyses. A false colour composite (FCC) of the image acquired is shown in Figure 2. As our main objective was to discriminate agricultural crops, all non-vegetation classes such as bare soil, roads, built-up and wetlands were eliminated from the classification process by preparing a crop mask based on the reference Land Use Planning Map-1999 available for the study area (Wegehenkel *et al*. 1999). Further, the within field non-crop features such as water body and built up areas were masked out from the analyses based on a vegetation mask generated by Normalized Difference Vegetation Index (NDVI) thresholding (Susaki, and Shibasaki 1999). The phenology of the crops in the HyMap image was quite variable and ranged from main shoot development to reproductive development.

2.2.2. *Crop spectral measurements*

Canopy level spectral measurements of alfalfa, winter barley, winter rape, winter wheat and winter rye were collected using an ASD FieldSpec JR spectroradiometer during the growing seasons 2002–2005. The spectroradiometer collects data in 1512 narrow spectral bands with bandwidth ranging from 1 nm in the visible–near infrared (VNIR) to 2 nm in the shortwave-infrared wavelength. Spectral measurements were collected at discrete point locations for each crop at regular intervals of 7–10 days during the entire growth cycle of each crop. At each measurement site, 50 reflectance measurements were taken by positioning the instrument's pistol grip at

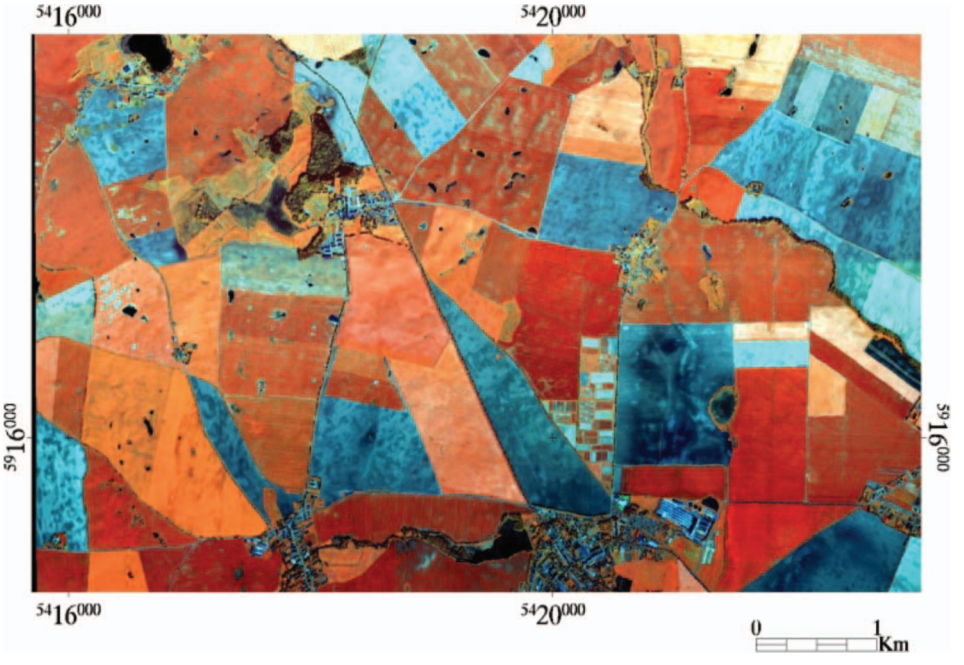

Figure 2. FCC of the HyMap image (R: 30, G: 20, B: 10) of the study area.

nadir view and using an 18° field of view at a height of about 1 m above the canopy. These 50 reflectance measurements were averaged to form a reflectance spectrum. Overall, 1350 reflectance spectra were collected for the crops selected. To avoid the impact of diurnal illumination changes, all the spectral measurements were collected during 11:00–13:00 h local noon time. The spectral data were calibrated with the reference measurements acquired simultaneously with a Barium sulphate ($BaSO_4$) white reference panel.

2.2.3. *Spectral library construction*

In order to evaluate the spectral matching of crops at various levels of spectral averaging (i.e. exemplar spectra generation) and the impact of number of samples for each crop type on the spectral matching, various spectral libraries were constructed from the field spectral database. At the highest level of spectral processing, spectral measurements of each crop from an entire growing season were averaged to form a single spectrum and were compiled as a spectral library and named SL1. The spectral library SL1 contained one reference spectrum for each crop per growing season. Similarly, all the 1350 spectral measurements were spectrally averaged and compiled into two other spectral libraries named SL2 and SL3 with 25 (5 samples for each crop) and 50 (10 samples for each crop) reference spectra, respectively, for each crop. In addition to this, all the 1350 reflectance measurements were as a spectral library named as SL4 without any spectral averaging. The number of spectral samples for each crop in the SL4 varied from 230 (winter rye) to 295 (winter wheat). To facilitate a direct comparison of wavelengths and reflectance values between image and library spectra, the spectral libraries were resampled to HyMap sensor spectral and radiometric resolutions using the spectral response function of the HyMap imaging sensor. The wavelengths (band centres) and full width half maxima (FWHM) of the HyMap imaging sensor were given as inputs and the spectral resampling was done using a Gaussian model with a FWHM equal to the band spacing.

2.2.4. *Selection of library search methods*

If the spectral samples in the spectral library are unique spectral features, then automatic detection and mapping of materials in the hyperspectral image should be possible. This requires the selection of an image classification algorithm which performs the material mapping in a spectral library search mode and is insensitive to brightness differences caused by illumination variations. Hence, the SAM classifier (Kruse *et al.* 1993) which performs image classification with a minimum of one reference spectrum for each crop in library search mode was selected for evaluating the HyMap image classification by searching through the library spectra. The SAM method labels pixels based on the lowest spectral angle differences between image and library spectra. Pixels further away than the user specified maximum angle threshold are left unclassified. Further, this method is insensitive to brightness differences caused by illumination changes. In addition to this, spectral matching of the image and library spectra with emphasis on the presence of spectral absorption features was evaluated using the SFF method (Clark *et al.* 1990a). The SFF method compares the library and image spectra by exploiting the spectral absorption features using a least-squares technique. The library spectra are matched with the image spectra after the continuum is removed from both datasets. The output from the SFF method is a set of gray level image pairs

known as scale and root mean square (RMS) error for each crop type. The brighter pixels in the scale image and darker pixels in the RMS image indicate better match to the reference materials. Scale values exceeding 1 indicate the possibility of incorrect reference endmembers or wavelength range used. The classification results were validated using reference data extracted from the Land Use Planning Map (Wegehenkel *et al*. 1999) available for the study area.

3. Results and analysis

3.1. HyMap image classification using the SAM method

Spectral discrimination of the crops in the HyMap image was carried out by varying the number of input reference spectra as per the spectral libraries SL1–SL4. Varying the number of reference spectra iteratively for each class changed the composition and distribution of classified pixels across the growing seasons. Figure 3 shows the classified images obtained from using the various spectral libraries constructed. When only one reference spectrum per crop type was used for library search (i.e. searching through SL1), the majority of the image pixels are left unclassified (results are not shown). However, when increasing the number of reference spectra per crop type to two and repeating the image classification by searching through the SL1, most of the image pixels were classified (Figure 3(a)).The majority of the pixels left unclassified (60%) are winter rape. The accuracy of the classification ranged from

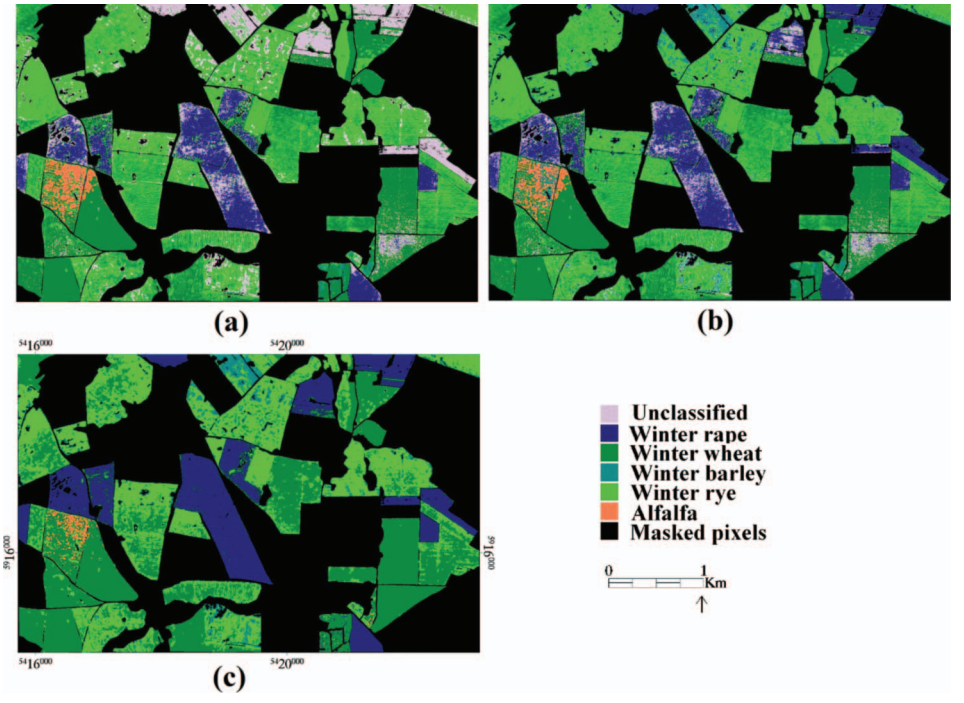

Figure 3. Classified image showing the crops selected. HYMap image was classified by library search through (a) spectral library SL1 including 2 reference spectra per crop, (b) spectral library SL2 (contained 5 reference spectra per crop), and (c) spectral library SL3 (contained 10 reference spectra per crop).

negligible (1%) to significant (71%; Table 1). As evident from Figure 3(a) and Table 1, with the exception of winter rape, majority pixels of all the crops are misclassified (as belonging to one crop or the other). For instance, most of the winter wheat pixels are labelled as winter rye, while the winter barley pixels are systematically misclassified as winter wheat. Remarkably, classified pixels of winter rape are accurate despite nearly one half of the area of winter rape left unclassified (Figure 3(a)). Further increase in the number of reference spectra per crop to five and repetition of the library search (i.e. searching through SL2) produced results almost similar to those obtained from using two reference spectra for each crop (see Figure 3(b) and Table 2). However, there is a decrease in the number of unclassified pixels of winter rape. Repetition of the classification by searching through SL3 only produced the results (see Figure 3(c) and Table 3) which are almost similar to those obtained from searching through SL2. However, major changes are the labelling of the previous unclassified pixels and the completeness of the classification performance by the winter rape.

Post-classification processing of screening out isolated single pixels and running a 3×3 majority filter on the classification results (obtained from searching through

Table 1. Contingency matrix showing accuracy assessment results obtained from the classification of HyMap image by spectral library search through SL1 using SAM method.

		Ground truth (pixels)					
	Class	Alfalfa	Winter barley	Winter rape	Winter rye	Winter wheat	Total
Classified image (pixels)	Unclassified	3	79	595	2	49	337
	Alfalfa	135	11	0	0	0	146
	Winter barley	12	13	0	2	8	35
	Winter rape	0	12	711	0	0	1,114
	Winter rye	95	156	9	189	299	748
	Winter wheat	505	982	23	73	339	1,922
	Total	750	1,253	1,338	266	695	4,302

Notes: Overall accuracy = 32%. Kappa coefficient = 0.18.

Table 2. Contingency matrix showing accuracy assessment results obtained from the classification of HyMap image by spectral library search through SL2 using SAM method.

		Ground truth (pixels)					
	Class	Alfalfa	Winter barley	Winter rape	Winter rye	Winter wheat	Total
Classified image (pixels)	Unclassified	1	61	189	0	5	165
	Alfalfa	95	7	0	0	0	102
	Winter barley	5	25	0	1	42	73
	Winter rape	0	11	1,132	0	0	1,234
	Winter rye	54	135	5	214	395	803
	Winter wheat	595	1,014	12	51	253	1,925
	Total	750	1,253	1,338	266	695	4,302

Notes: Overall accuracy = 40%. Kappa coefficient = 0.21.

Table 3. Contingency matrix showing accuracy assessment results obtained from the classification of HyMap image by spectral library search through SL3 using SAM method.

		Ground truth (pixels)					
	Class	Alfalfa	Winter barley	Winter rape	Winter rye	Winter wheat	Total
Classified image (pixels)	Unclassified	0	3	2	0	4	9
	Alfalfa	52	1	0	0	0	53
	Winter barley	1	32	0	1	35	69
	Winter rape	0	0	1,327	0	0	1,327
	Winter rye	42	89	2	140	346	619
	Winter wheat	655	1,128	7	125	310	2,225
	Total	750	1,253	1,338	266	695	4,302

Notes: Overall accuracy = 43%. Kappa coefficient = 0.22.

the SL2) yielded a classified image which is smooth and coherent (Figure 3(c)) indicating its potential for further studies to long-term reference spectral signature development. On the other hand, the spectral confusion as evident from the misclassifications of winter rye, winter barley and winter wheat enhanced to being mutually inclusive. This is evident from the completeness in the mislabelling of winter barley and winter wheat plots (Figure 3(c)). The classification of alfalfa exhibited an interesting spectral (mis)matching pattern. As evident from Figure 3, the pixels labelled as alfalfa are indeed alfalfa and there is no evidence on alfalfa occupying the pixels which belong to other crops. This observation indicates the likely case of the existence of exemplar spectral features for alfalfa which might have been modified by the presence of unidentified vegetation types such as grass in the alfalfa plots.

The final case of repeating the library search by using all the 1350 entries in the spectral library produced no additional gains in the classification performance but impractical post-classification processing (Yang and Tien 2010). Several hundreds of tiny and single pixel classes were accumulated in the classified image with no meaningful relation to the ground truth image. Therefore, results from the SL4 were discarded.

3.2. Classification using the SFF method

Because of the complexity of the output grey level images, the SFF method was applied only on the various combinations of reference spectra in SL1 and SL2. Examination of the numerous scale and RMS error images of the crops across the growing seasons and number of entries in the spectral libraries revealed the quantitative basis for the classification results obtained by the SAM method. Results from the SFF method confirm the randomness observed in the classification of winter barley, winter rye and winter wheat by the SAM method. The scale and RMS values of winter barley, winter rye and winter wheat ranged from 1.1 (from SL1) to 1.6 (from SL2) and 0.28 to 0.59, respectively. Typical scale and RMS image pairs of the crops obtained by the SFF using SL1 are shown in Figure 4. From Figure 4, it is evident that the scale values for winter barley (Figure 4(c)), winter rye (Figure 4(g)) and winter wheat (Figure 4(i)) exceed the theoretical upper limit of one for a valid spectral comparison (Clark *et al.* 1990a) indicating the inability of the field spectra of

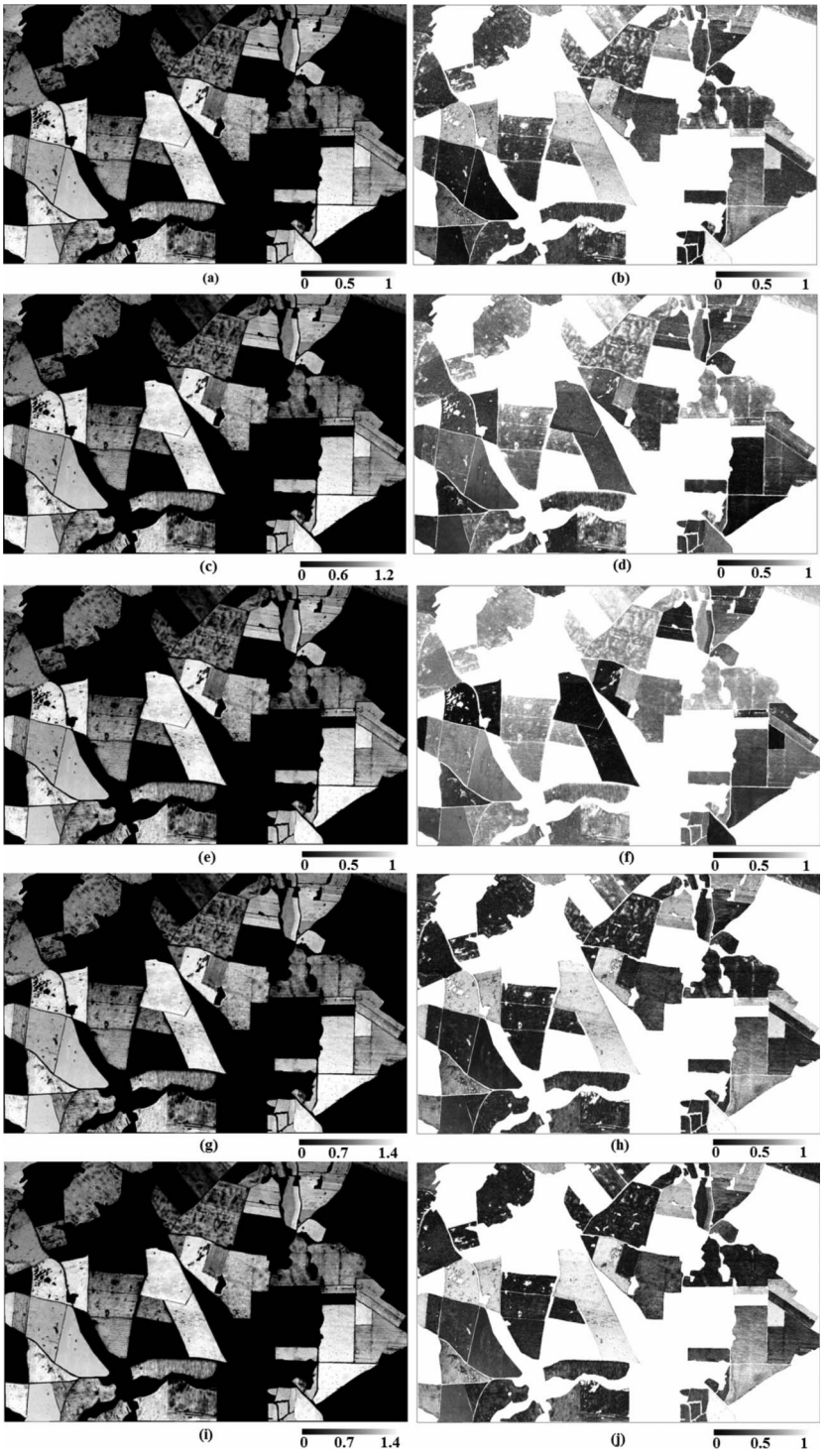

Figure 4. Scale and RMS images of alfalfa (a and b), winter barley (c and d), winter rape (e and f), winter rye (g and h) and winter wheat (i and j) from the SFF method.

these crops for spectral matching. This invalid spectral matching is also evident by the comparatively higher RMS error values. In contrast to that, winter rape exhibited an outstanding spectral matching with the image spectra while maintaining distinct spectral separation from the other crops. This is clearly evident from the higher scale values but less than 1 (Figure 4(e) and (f)) and the lowest RMS error values in the corresponding scale and RMS images for winter rape.

Further analysis of the 80 pairs of scale and RMS image pairs obtained by searching through the spectral library SL2 resulted in only the confirmation of the invalid range of the scale values as observed with the spectral library SL1. However, there are a limited number of scale images with values less than 1. However, the comparatively higher RMS values of these scale images rule out the validity of results. On the other hand, the maxima and minima of the scale and RMS values obtained from the various combinations of the spectral libraries SL1 and SL2 ranged from 0.8 to 1 and 0.013 to 0.028, respectively. This observation supports validity of the results obtained from the SFF method for winter rape (Figure 4(e) and (f)) and the exemplar spectral matching observed by using the SAM method. Interestingly, the RMS values of alfalfa are nearly close to those of the winter rape but with invalid scale values (Figure 4(a) and (b)).This observation explains the systematic under estimation of alfalfa pixels by the SAM method.

4. Discussion

State-of-the-art hyperspectral imaging systems provide reflectance data with spectral resolutions that are required for the purposes of studying material chemistry. Material identification by reference library search is an emerging approach of hyperspectral image classification. Leveraging the scientific understanding that many minerals exhibit unique spectral absorption features, previous studies have demonstrated the proof of the concept by automatic classification of airborne hyperspectral images for mineral identification mapping (Clark *et al*. 1990b). In these studies, an unknown spectrum is identified by simply matching the dominant absorption feature in its reflectance spectrum with those present in a spectral library. However, unlike minerals which exhibit characteristic absorption features, vegetation species show distinct spectral reflectance patterns driven by plant type, structure, phenology, and the presence and orientation of individual plant components (Price 1994, Cochrane 2000, Kumar *et al*. 2001, 2010, Kumar 2007). Therefore, vegetation species identification by spectral library search will more likely be a result of the existence of distinct shape of reflectance spectrum, often called exemplar spectra (Gomez 2002, Nidamanuri and Zbell 2010). These exemplar spectra permit integration of *in situ* reflectance measurements with airborne hyperspectral measurements for material identification and mapping.

Our experimental setup of collecting multi-season field spectral measurements independent of the time and location of the hyperspectral image acquisition made it possible to assess the existence of unique spectral signatures with potential for hyperspectral image classification. The observed consistency in the discrimination of winter rape demonstrates experimentally the fundamental principle of remote sensing which suggests the incorporation of reference spectral signatures for image classification (Campbell 2006).

A visual examination of the reflectance profiles of the crops selected indicates the presence of spectral similarity among cereals and a unique reflectance pattern for

winter rape and alfalfa (Figure 5). Especially, the visible reflectance pattern of winter rape is unique in its entirety, explaining the higher classification accuracy obtained from both the SFF and SAM methods. Adding to that, *in situ* reflectance spectrum of winter rape is qualitatively and quantitatively similar to the spectrum extracted from airborne HyMap image. These outstanding spectral features may be responsible for the discrimination of winter rape, and alfalfa by the SFF and SAM methods. The remarkably higher reflectance of winter rape in the red and green wavelengths indicates the reflectance of the characteristic yellow flowers of winter rape, which are the dominant canopy components for mature winter rape.

On the other hand, the finer spectral differences existing among the field spectra of cereal crops (Figure 5) are mainly evident by the apparent differential brightness values rather than the spectral variation, thus leading to negligible discrimination of winter barley, winter rye and winter wheat by the SFF and SAM methods. This is because both the SFF and SAM methods use shape of the reflectance spectrum for endmember identification (Mazer *et al*. 1988, Kruse *et al*. 2003). However, the SFF method quantifies similarity based on the position and depth of spectral absorption features, whereas the SAM method considers the overall shapes of reflectance spectra as measured by vector dot product (Price 1994).

In a similar study, Nidamanuri *et al*. (2007) reported an overall accuracy of about 90% in an experiment of supervised classification of Hyperion space-borne hyperspectral imagery by the SAM method for mapping four agricultural crops (paddy rice, cotton, sugarcane and chillies) using field spectra. As against our case of independent locations of field measurements and image acquisition, however, their study used field spectra that are collected from the same crop fields and concurrent to the image acquisition. The observed consistency in the lack of matching between field and image spectra for winter barley, winter rye and winter wheat by any of the methods closely follows the observations of Price (1994) and Cochrane (2000). After posing the question 'How unique are spectral signatures?', Price concludes that the spectral signatures of various vegetation species are not unique and that there is no one-to-one relationship between vegetation species and spectral signatures. By using leaf and branch level reflectance spectra for forest species, as against the use of laboratory spectra by previous studies, reported the lack of unique spectral signatures.

The plant-specific outstanding spectral feature of winter rape observed in this study supports the study reported by Andrew and Ustin (2006). They report unique identification and discrimination of perennial pepperweed from its co-occurring species using field reflectance measurements and airborne hyperspectral imagery. Furthermore, studies of Zomer *et al*. (2009), Ciraolo *et al*. (2006), Kutser *et al*. (2006) and Purkisand and Pasterkamp (2004) report successful automatic classification of airborne hyperspectral data for various wetland and submerged aquatic vegetation species using spectral libraries developed using *in situ* reflectance spectra. However, most of these studies used *in situ* reflectance spectra that were collected concurrent with the date of image acquisition and from the same locations. Contrary to this, we used spatially and temporally independent image and spectral measurements. There has been up to 6 years of time difference between the date of HyMap image acquisition and collection of spectral measurements, and an aerial distance of 100 km between the sites of spectral measurements and image acquisition. These wider spatio-temporal differences maintained in our experiment set the ideal

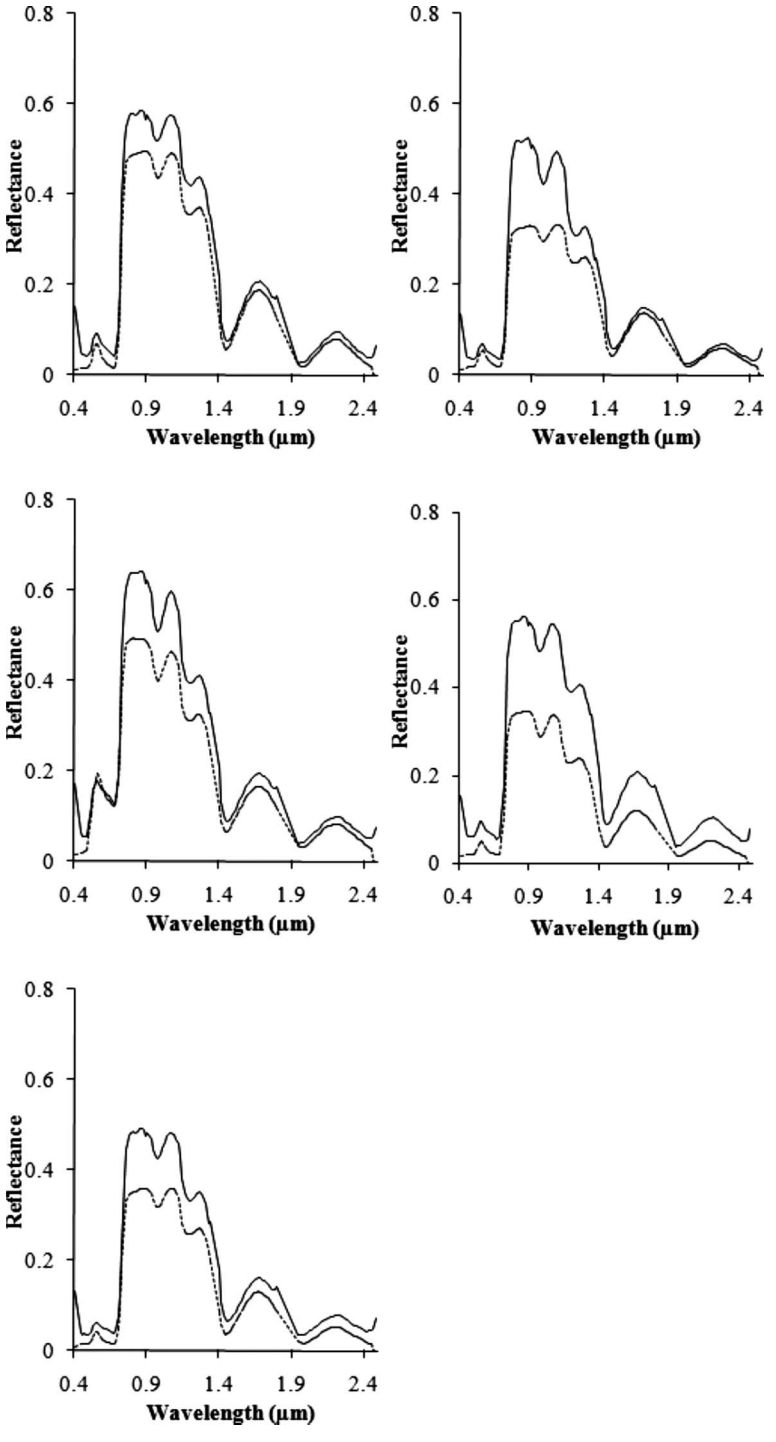

Figure 5. Field and image spectral signatures of the crops selected: (a) alfalfa, (b) winter barley, (c) winter rape, (d) winter rye and (e) winter wheat. Winter rape and alfalfa show an outstanding reflectance pattern in the visible and NIR wavelengths. Unique visible reflectance feature of winter rape is clearly evident. Solid line indicates image spectrum and dotted indicates field spectrum.

conditions for assessing uniqueness of spectral signatures and ensure free of being site-specific at least on a regional basis.

The observed consistency in the identification and classification of winter rape across seasons and independent of the location suggests the existence of an outstanding spectral signature for winter rape. This is an important observation in the context of the subjectivity in the current notion that unique spectral signatures may not exist for vegetation (Cochrane 2000), despite the theoretical possibility. Interestingly, the observed randomness in the spectral matching of winter barley, winter rye and winter wheat contributes to the notion of non-existence of unique spectral signatures. Based on these results, it can be inferred that the existence or non-existence of unique spectral signatures cannot be generalized across vegetation but is case specific. The crops (or vegetation), which exhibit this feature of spectral uniqueness, may become potential candidates for automated mapping using hyperspectral imagery. We, therefore, recommend the review of ongoing efforts of building spectral libraries (e.g. Clark *et al*. 2007, Baldridge *et al*. 2009, Huenia *et al*. 2009) to maintain a collaborating open-end vegetation reference spectral library whose entries are unique spectral signatures. The results of this study indicate that winter rape is one such potential candidate.

5. Conclusions

The primary purpose of this research was to assess the relevance of identifying and assessing characteristic spectral data for material mapping by spectral library search. Spatio-temporal spectral matching and classification of a historical HyMap image for five agricultural crops suggest the existence of a unique spectral matching between image and field spectra for certain crop species. The matching of the field reflectance measurements of winter rape with the image spectra by magnitude and direction, consistent across seasons, indicates the existence of physiologically unique spectral signature for winter rape against the crops considered. This unique spectral behaviour may be further studied for assessing the possibility of automatic mapping of winter rape across space and time. The randomness observed in the classification of winter rye, winter wheat and winter barley suggests that reflectance spectra of some crop species may closely approximate another similar group of crop species even in high resolution spectral data.

References

Andrew, M.E. and Ustin, S.L., 2006. Spectral and physiological uniqueness of perennial pepperweed (*Lepidium latifolium*). *Weed Science*, 54, 1051–1062.

Baldridge, A.M., *et al*., 2009. The ASTER spectral library version 2.0. *Remote Sensing of Environment*, 113, 711–715.

Bojinski, S., Schläpfer, D., and Itten, K., 2003. SPECCHIO: a spectrum database for remote sensing applications. *Computers & Geosciences*, 29, 27–38.

Brown, D.J., 2007. Using a global VNIR soil-spectral library for local soil characterization and landscape modeling in a 2nd-order Uganda watershed. *Geoderma*, 140, 444–453.

Brown, D.J., *et al*., 2006. Global soil characterization with VNIR diffuse reflectance spectroscopy. *Geoderma*, 132, 273–290.

Bue, B., Merényi, E., and Csathó, B., 2010. Automatic labeling of materials in hyperspectral imagery. *IEEE Transactions on Geoscience and Remote Sensing*, 48, 4059–4070.

Bue, B.D. and Merenyi, E., 2010. Using spatial correspondences for hyperspectral knowledge transfer: evaluation on synthetic data. *In*: *Proceedings of the 2nd workshop on hyperspectral image and signal processing: evolution in remote sensing (WHISPERS)*, 14–16 June 2010, Reykjavik.

Campbell, J.B., 2006. *Introduction to Remote Sensing*. 4th ed. New York: Guilford Publications.

Camps-Valls, G. and Bruzzone, L., 2005. Kernel-based methods for hyperspectral image classification. *IEEE Transactions on Geoscience and Remote Sensing*, 43, 1351–1362.

Chang, C.I., 2000. An information theoretic-based approach to spectral variability, similarity and discriminability for hyperspectral image analysis. *IEEE Transactions on Information Theory*, 46, 1927–1932.

Ciraolo, G., *et al*., 2006. The classification of submerged vegetation using hyperspectral MIVIS data. *Annals of Geophysics*, 49, 287–294.

Clark, R.N., Gallagher, A.J., and Swayze, G.A., 1990a. Material absorption band depth mapping of imaging spectrometer data using the complete band shape least-squares algorithm simultaneously fit to multiple spectral features from multiple materials. *In*: *Proceedings of the third airborne visible/infrared imaging spectrometer (AVIRIS) workshop*. Pasadena, CA: JPL Publication, 90-54.

Clark, R.N., *et al*., 1990b. High spectral resolution reflectance spectroscopy of minerals. *Journal of Geophysical Research*, 95, 12653–12680.

Clark, R.N., *et al*., 2007. *USGS digital spectral library splib06a: U.S. Geological Survey*. Digital Data Series 231.

Cochrane, M.A., 2000. Using vegetation reflectance variability for species level classification of hyperspectral data. *International Journal of Remote Sensing*, 21, 2175–2087.

Demir, B. and Erturk, S., 2007. Hyperspectral image classification using relevance vector machines. *IEEE Geoscience and Remote Sensing Letters*, 4, 586–590.

Felde, G.W., *et al*., 2003. Analysis of Hyperion data with the FLAASH atmospheric correction algorithm. *In*: *Proceedings of the IEEE international geoscience and remote sensing symposium IGARSS '03*. Vol. 1. New York City: IEEE, 90–92.

Gomez, R.B., 2002. Hyperspectral imaging: a useful technology for transportation analysis. *Optical Engineering*, 41, 21–37.

Herold, M., *et al*., 2004. Spectrometry for urban area remote sensing – development and analysis of a spectral library from 350 to 2400 nm. *Remote Sensing of Environment*, 91, 304–319.

Huenia, A., *et al*., 2009. The spectral database SPECCHIO for improved long term usability and data sharing. *Computers & Geosciences*, 35, 557–565.

Kaewpijit, S., Le Moigne, J., and El-Ghazawi, T., 2003. Automatic reduction of hyperspectral imagery using wavelet spectral analysis. *IEEE Transactions on Geoscience and Remote Sensing*, 41, 863–871.

Knorn, J., *et al*., 2009. Land cover mapping of large areas using chain classification of neighboring Landsat satellite images. *Remote Sensing of Environment*, 113, 957–964.

Kokaly, R.F., King, T.V.V., and Livo, K.E., 2008. *Airborne hyperspectral survey of Afghanistan 2007: flight line planning and HyMAP data collection*. Reston, VA: U.S. Geological Survey, USGS Afghanistan Project Product No. 186.

Kruse, F.A. and Perry, S.L., 2009. Improving multispectral mapping by spectral modeling with hyperspectral signatures. *Journal of Applied Remote Sensing*, 3, 033504.

Kruse, F.A., *et al*., 1993. The Spectral Image Processing System (SIPS) – interactive visualization and analysis of imaging spectrometer data. *Remote Sensing of Environment*, 44, 145–163.

Kumar, L., 2007. A comparison of reflectance characteristics of some Australian eucalyptus species based on high spectral resolution data – discriminating using the visible and NIR regions. *Journal of Spatial Science*, 52, 51–64.

Kumar, L., *et al*., 2001. Imaging spectrometry and vegetation science. *In*: F. van de Meer and S.M. de Jong, eds. *Imaging spectrometry*. Dordrecht: Kluwer Academic Press, 111–155.

Kumar, L., Skidmore, A.K., and Mutanga, O., 2010. Leaf level experiments to discriminate between eucalyptus species using high spectral resolution reflectance data: use of derivatives, ratios and vegetation indices. *Geocarto International*, 25, 327–344.

Kruse, F.A., *et al*., 2003. Evaluation and validation of EO-1 Hyperion for mineral mapping. *IEEE Transactions on Geosciences and Remote Sensing*, 41, 1388–1400.

Kutser, T., Millerb, I., and Jupp, L.B., 2006. Mapping coral reef benthic substrates using hyperspectral space-borne images and spectral libraries. *Estuarine, Coastal and Shelf Science*, 70, 449–460.

Landgrebe, D., 2002. Hyperspectral image data analysis as a high dimensional signal processing. *IEEE Signal Processing Magazine*, 19, 17–28.

Liu, Y., *et al*., 2010. Building topographic subspace model with transfer learning for sparse representation. *Neurocomputing*, 73, 1662–1668.

Mazer, A.S., *et al*., 1988. Image processing software for imaging spectrometry analysis. *Remote Sensing of Environment*, 24, 201–210.

Nidamanuri, R.R., Garg, P.K., and Ghosh, S.K., 2007. Development of an agricultural crops spectral library and classification of crops at cultivar level using hyperspectral data. *Precision Agriculture*, 8, 173–185.

Nidamanuri, R.R. and Zbell, B., 2010. A method for selecting optimal spectral resolution and comparison metric for material mapping by spectral library search. *Progress in Physical Geography*, 34, 47–58.

Nidamanuri, R.R. and Zbell, B., 2011. Normalized spectral similarity score (NS^3) as an efficient spectral library searching method for hyperspectral image classification. *IEEE Journal of Selected Topics in Applied Earth Observations and Remote Sensing*, 4, 226–240.

Plaza, A., *et al*., 2005. Dimensionality reduction and classification of hyperspectral image data using sequences of extended morphological transformations. *IEEE Transactions on Geoscience and Remote Sensing*, 43, 466–479.

Price, J.C., 1994. How unique are spectral signatures? *Remote Sensing of Environment*, 49, 181–186.

Purkisand, S.J. and Pasterkamp, R., 2004. Integrating in situ reef-top reflectance spectra with Landsat TM imagery to aid shallow-tropical benthic habitat mapping. *Coral Reefs*, 23, 5–20.

Rajan, S., Ghosh, J., and Crawford, M., 2006. Exploiting class hierarchies for knowledge transfer in hyperspectral data. *IEEE Transactions on Geoscience and Remote Sensing*, 44, 3408–3417.

Rajan, S., Ghosh, J., and Crawford, M.M., 2008. An active learning approach to hyperspectral data classification. *IEEE Transactions on Geoscience and Remote Sensing*, 46, 1231–1242.

Ratle, F., Camps-Valls, G., and Weston, J., 2010. Semisupervised neural networks for efficient hyperspectral image classification. *IEEE Transactions on Geoscience and Remote Sensing*, 48, 2271–2282.

Shepherd, K.D. and Walsh, M.G., 2002. Development of reflectance spectral libraries for characterization of soil properties. *Soil Society of America Journal*, 66, 988–998.

Stephani, H., *et al*., 2010. Wavelet-based dimensionality reduction for hyperspectral THz imaging. *Terahertz Science and Technology*, 3, 117–129.

Susaki, J. and Shibasaki, R., 1999. Crop field extraction method based on texture analysis and automatic threshold determination. *In*: Proceedings of the *IEEE international geoscience and remote sensing symposium, IGARSS'99*, 28 June–02 July 1999, Hamburg.

Van der Meer, F., 2005. The effectiveness of spectral similarity measures for the analysis of hyperspectral imagery. *International Journal of Applied Earth Observations and Geoinformation*, 8, 3–17.

Wang, J. and Chang, C.I., 2006. Independent component analysis based dimensionality reduction with applications in hyperspectral image analysis. *IEEE Transactions on Geoscience and Remote Sensing*, 44, 1586–1588.

Waske, B. and Benediktsson, J.A., 2007. Fusion of support vector machines for classification of multisensor data. *IEEE Transactions on Geoscience and Remote Sensing*, 45, 3858–3866.

Wegehenkel, M., *et al*., 1999. Simulation tool for the evaluation of agricultural productivity (STEAP (Ertragspotential). *In*: *ProSmart-Forschungs-Endbericht (DLR Förderkennzeichen: 50EE9816), Daimler Chrysler Aerospace, Dornier Satellittensysteme*, Dok. No.: EB-DSS-REP-0001: S. 11/1–11/62.

Yang, X. and Tien, D., 2010. An automated image analysis approach for classification and mapping of woody vegetation from digital aerial photograph. *World Review of Science, Technology and Sustainable Development*, 7, 13–23.

Zomer, R.J., Trabucco, A., and Ustin, S.L., 2009. Building spectral libraries for wetlands land cover classification and hyperspectral remote sensing. *Journal of Environmental Management*, 90, 2170–2177.